Applied Physics A (2020)126:551
https://doi.org/10.1007/s00339-020-03727-8

Applied Physics A
Materials Science & Processing

Detailed investigation of optical linearity and nonlinearity of nanostructured Ce-doped CdO thin films using Kramers–Kronig relations

V. Ganesh[1] · L. Haritha[2] · H. Elhosiny Ali[1,3] · A. M. Aboraia[3,4] · Yasmin Khairy[3] · H. H. Hegazy[1,3] · V. Butova[4] · Alexander V. Soldatov[4] · H. Algarni[1] · H. Y. Zahran[1,5] · I. S. Yahia[1,5,6]

Received: 22 April 2020 / Accepted: 14 June 2020

Abstract
Sol–gel-assisted spin coating technique has been employed to deposit Ce-doped cadmium oxide films (CdO) thin films on a glass substrate. Structural analysis carried out by XRD revealed that the films are polycrystalline and crystallize in a cubic structure. The preferential directions for the CdO growth are (2 0 0), and (2 1 0) and doping of Ce ions inhibits the growth. In addition to XRD, Raman analysis also supports the crystalline phase with no impurities. Using the Kramers–Kronig relations, the dispersion relation is evaluated from which the refractive index and the absorption coefficient were derived. The deposited doped and pure CdO films are highly transparent. The energy gap values of pure and doped CdO films are in the range of 2.2–4.2 eV, making them suitable for optoelectronic applications. The lower values of '*n*' and '*k*' are making the films most significant. The dielectric constant and nonlinear optical properties showed an increasing tendency on doping Ce ions into CdO films.

Keywords Ce-doped CdO · Nanostructured thin films · Sol–gel/spin coating technique · Bandgap analysis · Linear/nonlinear optical parameters

1 Introduction

Transparent conducting oxides are at the center of research for a long time and continues to attract researchers for their applications in thin films solar cells, displays, opto-electrical diodes, circulatory optical waveguides [1–3], sensors, etc. Hence TCOs have widened the area of investigation where researchers have focused on exotic dopants to improve the critical properties of a TCO, i.e., optical transparency and electrical conductivity. A wide variety of preparation and characterization techniques were adopted to study the properties of these TCOs.

From the literature survey, it is well understood that amongst all available TCOs, CdO has gained considerable attention for applications in optoelectronic devices. Cadmium oxide (CdO) is an n-type semiconductor with an optical bandgap of 2.2 eV [4–6], which crystallizes in a cubic structure. CdO makes itself favorable for a wide range of applications in flat panel displays, photodiodes, transparent electrodes, photovoltaic solar cells, optoelectronic devices [7, 8]. Outstanding excellent optical and electrical properties have been provided by the process of doping CdO films. This

✉ Yasmin Khairy

[1] Advanced Functional Materials and Optoelectronic Laboratory (AFMOL), Department of Physics, Faculty of Science, King Khalid University, P.O. Box 9004, Abha, Saudi Arabia

[2] Department of Physics, Telangana University, P.O. Box 503101, Nizamabad, Telangana State, India

[3] Physics Department, Faculty of Science, Zagazig University, Zagazig 44519, Egypt

[4] The Smart Materials Research Institute, Southern Federal University, Sladkova 178/24, Rostov-on-Don 344090, Russia

[5] Nanoscience Laboratory for Environmental and Bio-medical Applications (NLEBA), Semiconductor Lab, Physics Department, Faculty of Education, Ain Shams University, Roxy, Cairo 11757, Egypt

[6] Research Center for Advanced Materials Science (RCAMS), King Khalid University, P.O. Box 9004, Abha 61413, Saudi Arabia

Published online: 24 June 2020

has been proved when CdO is doped with metal and rare earth ions like La, Al, In, Ga, Eu, Ce, Sm, etc. [9–13]. The authors have studied the optical and non-linear properties of La-doped CdO films and presented the results [14].

However, there is not much literature available on cerium-doped CdO films. Thus, it is proposed to focus on the properties of Ce-doped films in this paper. The dopant cerium- (Ce^{4+}, Ce^{3+}) has an ionic radius of 0.092 and 0.103 nm, which are in comparison with that of Cd^{+2}, which is 0.097 nm. Cerium easily substitutes Cd^{+2} ions and increases electrical conduction. Moreover, Ce^{3+} possesses shielded 4f levels, which permit several well-defined narrow optical transitions among spin–orbit levels and consequently split the bandgap of CdO into sub-gaps. For this reason, Ce^{3+} is generally doped or associated with CdO to enhance the luminescence efficiency by energy transfer processes, and this topic is becoming an exciting area of research for developing electronic and optical applications like sensors, light-emitting phosphors or flat panel displays. High-quality deposition methods have been adopted by many researchers to deposit excellent CdO films on various crystalline, amorphous, and organic substrates. Magnetron sputtering [15], pulsed laser deposition [16], spray pyrolysis [17], chemical vapour deposition [18], electro-spinning [19], and vacuum evaporation [20] have been used to deposit pure and doped CdO films.

In the present paper, it is aimed to deposit pure and Ce-doped CdO films using a sol–gel-assisted spin coating technique and study the structural, morphological, linear, and non-linear optical properties of the films. The optical constants n and k are derived using Kramers–Kronig relations, which are simple and accurate. There is not much literature available on Ce-doped CdO film where optical constants are evaluated from Kramers–Kronig relations. Thus, it is worthwhile to investigate the linear and non-linear optical properties of Ce-doped CdO films using Kramers–Kronig relations.

2 Experimental details

2.1 Fabrication of nanostructured Ce-doped CdO films

The technique adopted to deposit Ce-doped CdO films is the sol–gel-assisted spin coating on cleaned glass substrates. The starting materials used are cadmium acetate and cerium chloride, which are of high quality purchased from Sigma Aldrich company. Cadmium acetate Cd $(CH_3COO)_2{\cdot}2H_2O$ and $CeCl_3$ are dissolved in 2-methaoxy ethanol to form the precursor solution. This mixture is stirred continuously on a magnetic stirrer at a specific temperature of 60 °C to obtain a homogeneous solution. To obtain sol, monoethanolamine (MEA) is added and stirred for an hour. After obtaining a clear solution, the sol is kept aside for 48 h to form a gel. This has been used to coat on the substrates using a spin coater operated at 1000 rpm for 50 s. Thus, deposited films are thermally treated to remove any organic residues. The same procedure is repeated, and the appropriate amount of $CeCl_3$ is added to obtain 3, 5, and 7% films. Afterward, annealing at 450 °C for 2 h was carried out for all the films.

2.2 Characterization techniques

Shimadzu LabX X-ray diffractometer equipped with CuK_α radiation operated at a wavelength of 6000 A° is used to record the X-ray patterns to understand the structure of the films.

The Raman spectra of the films are recorded using TS, DXR FT-Raman spectrometer in the range of 200–2000 cm^{-1}.

The surface morphology of the Ce-doped CdO films was investigated using an atomic force microscope [NT-MDT, Next (Russia)].

The optical properties (transmittance, reflectance, and absorbance) are obtained from a spectrophotometer JASCO UV–VIS–NIR-570.

2.3 Kramers–Kronig method and equations

The Kramers–Kronig relations are purely mathematical relations that are used to calculate the real part from the imaginary and imaginary from the real. These relations are satisfied by many physical parameters like susceptibility and optical dispersion relation. From the dispersion relation, the expression for refractive index '*n*' and extinction coefficient '*k*' is evaluated [21]. The values of *T* and *R* are the transmittance and reflectance of the film, which will be known in the further sections.

$$n(\omega) = \frac{1 - R(\omega)}{1 + R(\omega) - 2\sqrt{R(\omega)}\cos\phi(\omega)}, \tag{1}$$

$$k(\omega) = \frac{2\sqrt{R(\omega)}\sin\phi(\omega)}{1 + R(\omega) - 2\sqrt{R(\omega)}\cos\phi(\omega)}, \tag{2}$$

where

$$\phi(\omega) = \frac{-\omega}{\pi}\int_0^\infty \frac{\ln R(\omega') - \ln R(\omega)}{\omega'^2 - \omega^2}\mathrm{d}\omega'. \tag{3}$$

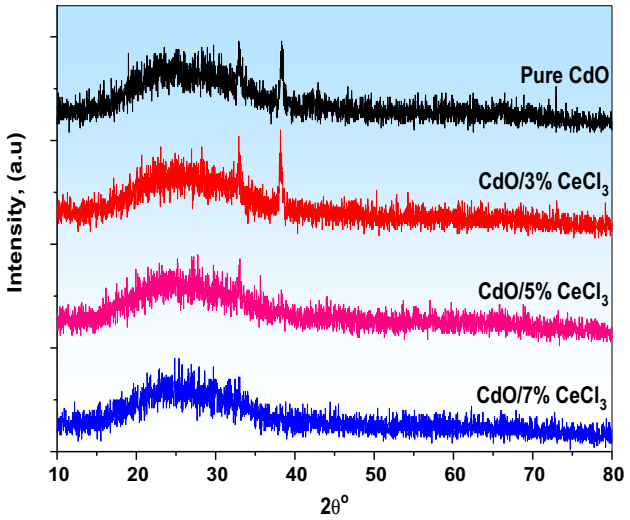

Fig. 1 Diffraction peaks of pure and Ce-doped (3, 5, and 7%) CdO nanostructured films

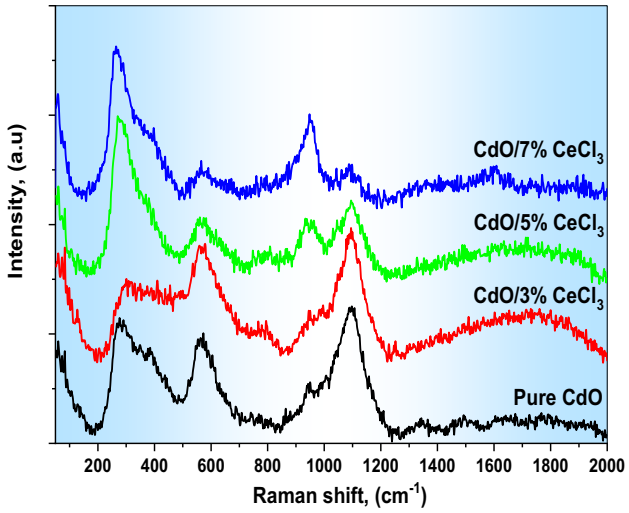

Fig. 2 Raman spectra pure and Ce-doped (3, 5, and 7%) CdO nanostructured films

3 Results and discussions

3.1 XRD patterns of nanostructured Ce-doped CdO films

Figure 1 shows the diffraction peaks of pure and Ce-doped (3, 5, 7%) CdO films in the range of 10–80°. The peaks with maximum peaks are observed at angles which are in correspondence with the earlier reported data. The preferential growth of the films is observed in the (200) and (210) directions. Moreover, as the doping concentration of Ce content increases, the growth of CdO is inhibited up to 3% concentration of doping. This may be attributed to the reason that the Ce atoms occupy the sites of Cd- in the CdO lattice, thereby inhibiting the growth. Literature reports are also in agreement with the results obtained by the authors [22].

3.2 Raman analysis of nanostructured Ce-doped CdO films

The Raman spectra of pure and Ce-doped CdO films in the range of 200–2000 cm^{-1} are displayed in Fig. 2. The first high intense Raman peak is observed at around ~ 289 cm^{-1}, and the shift in the peak is observed on doping Ce. The reason for this peak is attributed to combination of the transverse acoustic and optical phonon (TA + TO) modes of CdO thin films [23]. The intensity of the peak increases in Ce-doped CdO films. The second peak observed at 590 cm^{-1}, whose intensity decreases on doping. The next peak at 950 cm^{-1} is of less intensity for pure CdO films; whereas, the intensity becomes maximum for higher dopant concentration. The intensity of the peak, which is observed at 1100 cm^{-1}, decreases drastically upon doping. There is no signature of impurity observed in the Raman spectra and strongly supports the XRD analysis. The peak observed at the particular wavenumbers is in correspondence with the data available in the literature [24].

3.3 Morphological characterization of nanostructured Ce-doped CdO films

The optical and electrical properties generally depend on the morphology of the samples. Therefore, the study of morphology is worthwhile, and thus the morphologies of the samples are studied and are shown in Fig. 3. From the AFM images, it is observed that the grain size decreases with the increase in doping up to 3% doping concentration of cerium and then increases, which is in correlation with XRD analysis (Table 1).

3.4 Linear optical analysis of nanostructured Ce-doped CdO films based on the Kramers–Kronig analysis

The spectrum of transmittance, absorbance, and reflection in the range of (280–1000 nm) is shown in Fig. 4a–c. In Fig. 4a, the variation of transmittance with wavelength is depicted. The results emphasize that on adding Ce to CdO films, the transmittance is affected. It shows an increasing tendency with the increase in doping concentration. This is because of the smooth surfaces of the films, which scatter less amount of light. The percentage of transmittance is almost 80% for the film (3% Ce-doped CdO) in the visible region. Similar results are obtained by Mohammed et al. [22] when Ce-doped CdO films are prepared by spray pyrolysis technique. Hence, the deposited films

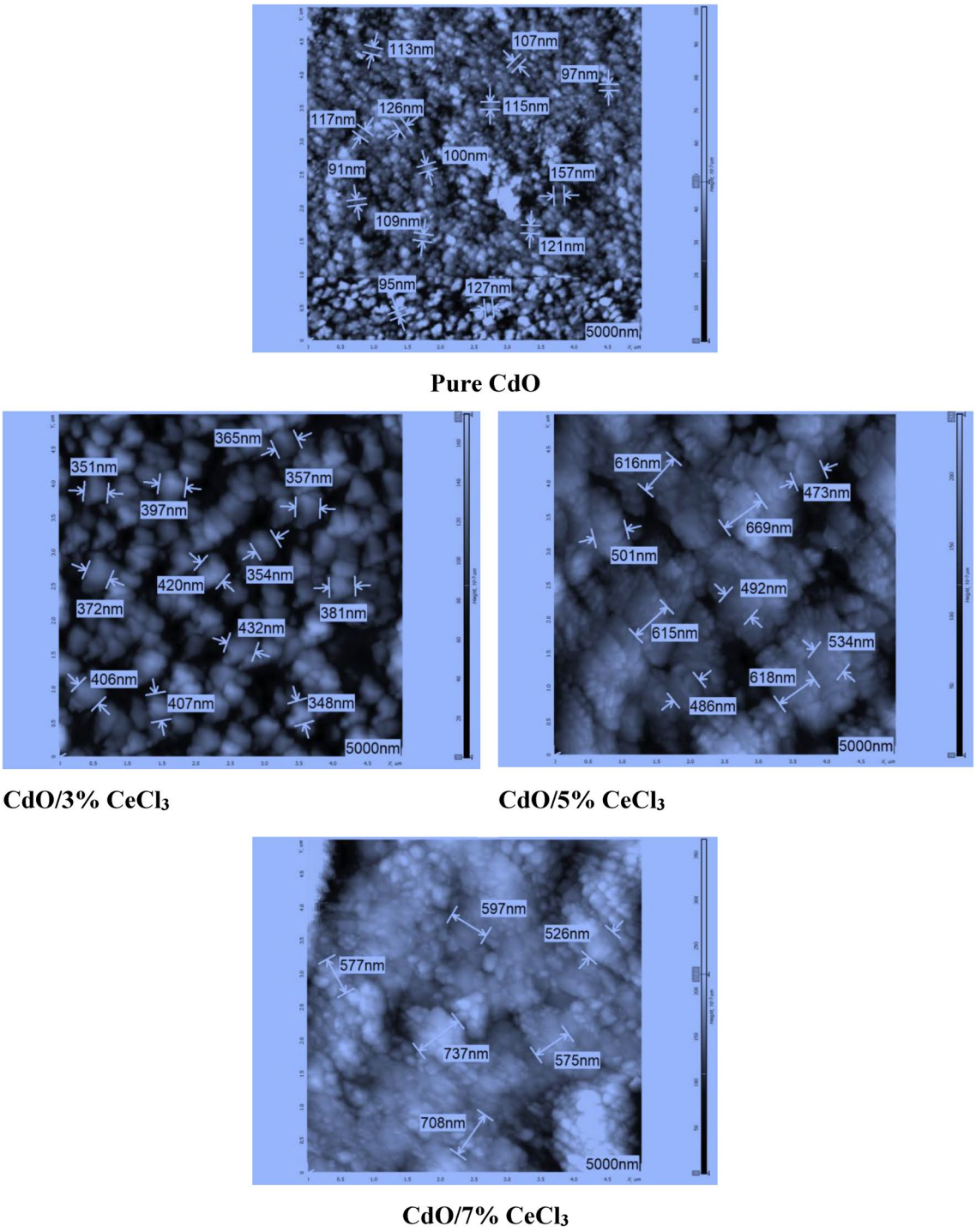

Fig. 3 AFM images of pure and Ce-doped (3, 5, and 7%) CdO nanostructured films

are more favorable for optoelectronic devices. The absorbance of the pure and Ce-doped CdO films is displayed in Fig. 4b. This shows a decreasing tendency at the shorter wavelength and is almost flat for all the films at higher wavelengths. From Fig. 4c, the reflectance is plotted as the function of wavelength. It is known from the figure that the reflectance is less in the visible region when compared at higher wavelengths. It is also inferred that the reflectance increases with an increase in doping of Ce ions into the CdO lattice.

The absorption coefficient is given by ($a = 4\pi k/\lambda$) at the essential edge is obtained utilizing the band-to-band

Table 1 Surface morphological and grain size analysis of nanostructured Ce-doped CdO thin films

Materials	Mean, the mean values of the grain size, (nm)	R_a, the arithmetical mean deviation of the profile	R_q, root-mean-square deviation of the profile	R_{sk}, skewness of profile	Rku, Kurtosis of profile
Pure CdO	113	37.827	46.182	0.235	2.296
ZnO/3% Ce	345	38.785	51.813	1.315	4.425
ZnO/5% Ce	382	32.354	40.046	0.804	2.806
ZnO/7% Ce	620	36.035	44.054	0.676	2.401

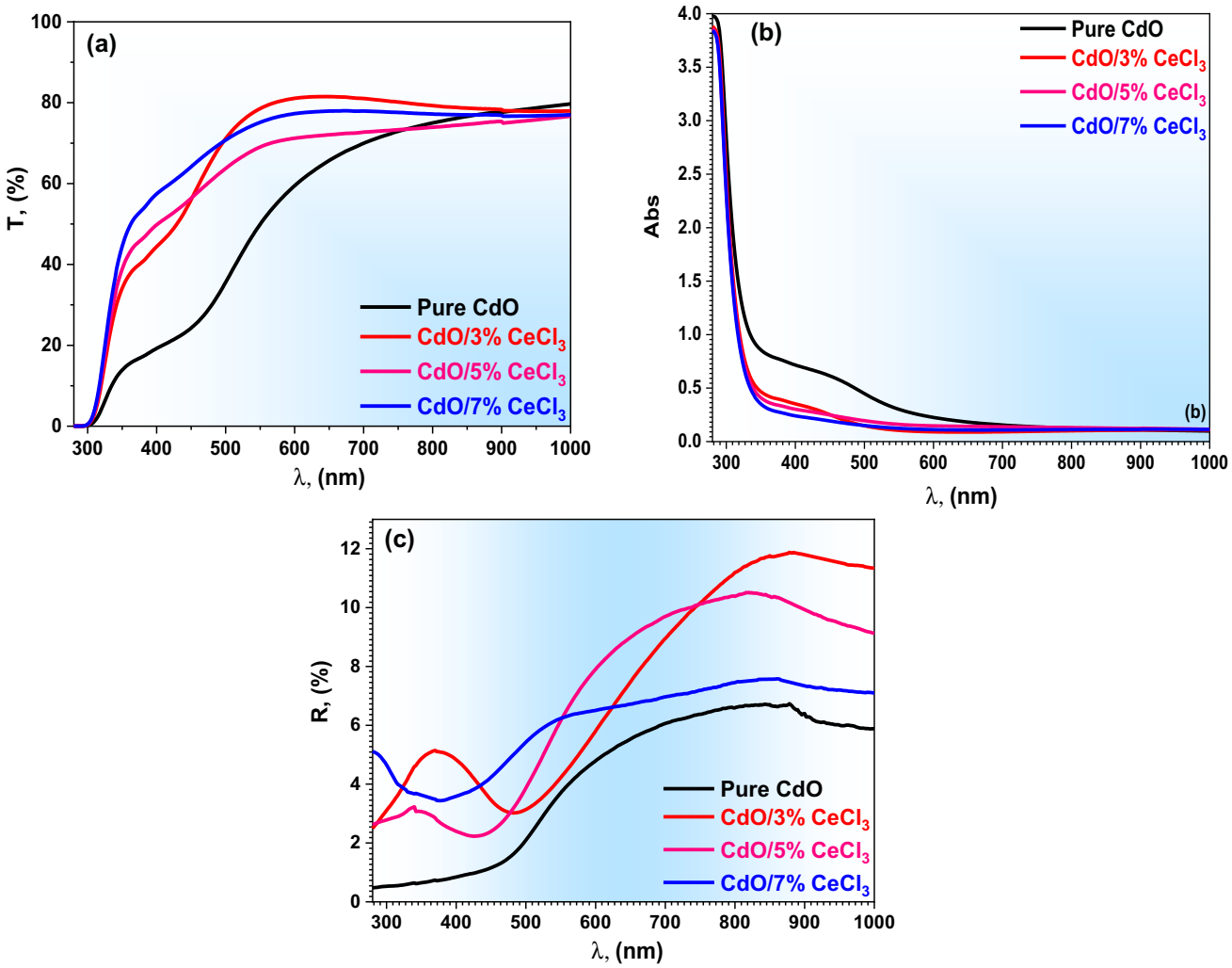

Fig. 4 **a–c** Transmission, absorption, and reflection graphs of pure and Ce-doped (3, 5, 7%) CdO nanostructured films, respectively

transition. The absorption coefficient pursues the accompanying condition [25]:

$$(\alpha E)^h = Q\left(E - E_g\right), \tag{4}$$

where E is the photon energy, Q is a constant, E_g is the energy gap, and h is a constant which decides the kind of electronic transitions. h is assumed to be 2 for the direct transition, and h assumes to be 1/2 for the indirect transition. The linear parts of the curves drawn from $(\alpha h\upsilon)^{1/2}$ verses $h\vartheta$ give the energy gap of the deposited pure and Ce-doped CdO films (see Fig. 5). From the graph, it is understood that the energy gap increases with an increase in the dopant concentration of Ce ions. Here are two energy gap blocks observed in the figure; in both the cases, band gap increases with an increase in dopant concentration. The energy gap

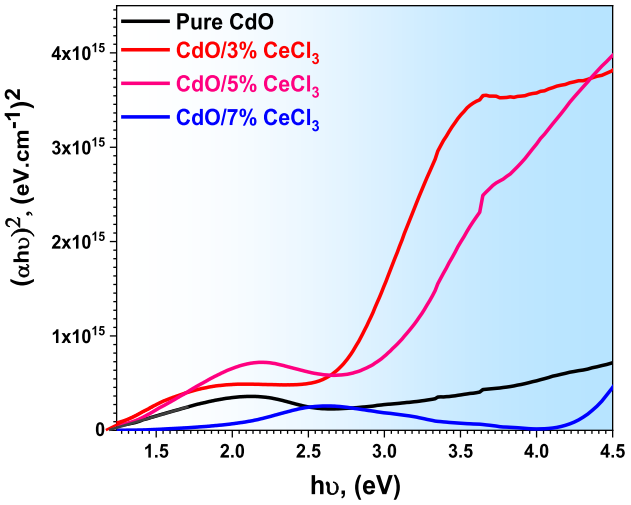

Fig. 5 Bandgap studies of pure and Ce-doped (3, 5, and 7%) CdO nanostructured films

of Ce-doped CdO film is larger than undoped film, and it may be attributed to the Burstein–Moss shift [12]. The energy gaps of pure and doped films are in the range of (2.1–4.2 eV), which is in correlation with the data available in the literature [4–6]. Similar behavior and the energy gap values are also presented in various reports [24].

The most significant factors refractive index '*n*' and extinction coefficient '*k*' are evaluated in the whole wavelength range by adopting the Kramers–Kronig method using the equations discussed in Sect. 2.3 [21]. (values for *T* and *R* are taken from Fig. 4). The refractive index and absorption index as a function of wavelength are depicted in Fig. 6a, b. The increase in the '*n*' values is observed in the visible region, which may be due to normal dispersion. In contrast, at shorter wavelengths, the value is almost 1 (at 300 nm, for all dopant concentrations). The lower value of the refractive index from 1 to 1.7 makes them favorable for optical applications in devices. The absorption index, which is a key factor in deciding the films for various applications, is studied as a function of wavelength. The lower values of *k* (0.2–0.6) indicate that the films are free from defects.

The electron excitation and optical properties of the material are given by the dielectric constant $\varepsilon = \varepsilon_r + i\varepsilon_i$. By knowing the values of *k* and *n*, ε_r and ε_i can be evaluated from the following equations [26]

$$\varepsilon_r = n^2 - k^2, \tag{5}$$

$$\varepsilon_i = 2nk. \tag{6}$$

Hence, the dielectric constant and real part of the dielectric constant are plotted as a function of wavelength in Fig. 7a, b. As the doping concentration of Ce ions is increased, the dielectric constant increases. The doping of Ce ions in the CdO films affects the dielectric properties significantly in the visible region. The real part of the dielectric constant also experiences the significant effect of doping in the visible and UV region. The lower values of 0.8–2.4 make the films fit into many optoelectronic devices.

Optical conductivity is calculated from the equation $\sigma_{opt} = \frac{\alpha nc}{4\pi}$, α being absorption coefficient, *n* being the refractive index and *c* is the speed of light (3×10^8m/s). The optical conductivity of pure and Ce-doped CdO films is displayed in Fig. 8a. It is noticed that the optical conductivity is increased with an increase in dopant concentration. The electrical conductivity of the present material is calculated

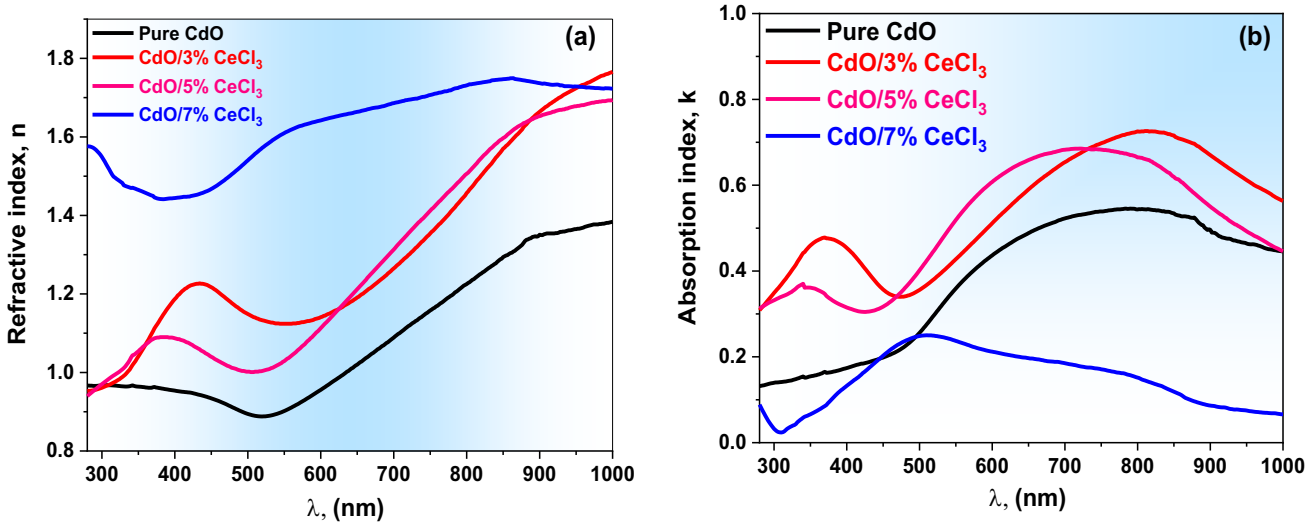

Fig. 6 **a**, **b** Refractive index and absorption index graphs of pure and Ce-doped (3, 5, and 7%) CdO nanostructured films

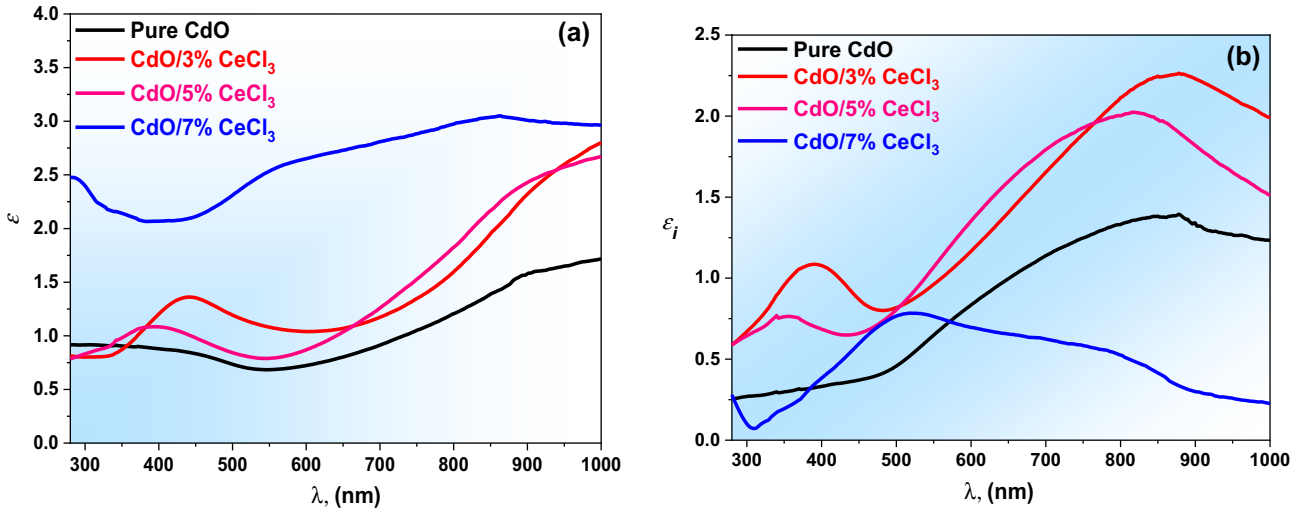

Fig. 7 **a**, **b** The dielectric constant and real part of the dielectric constant of pure and Ce-doped (3, 5, and 7%) CdO nanostructured films

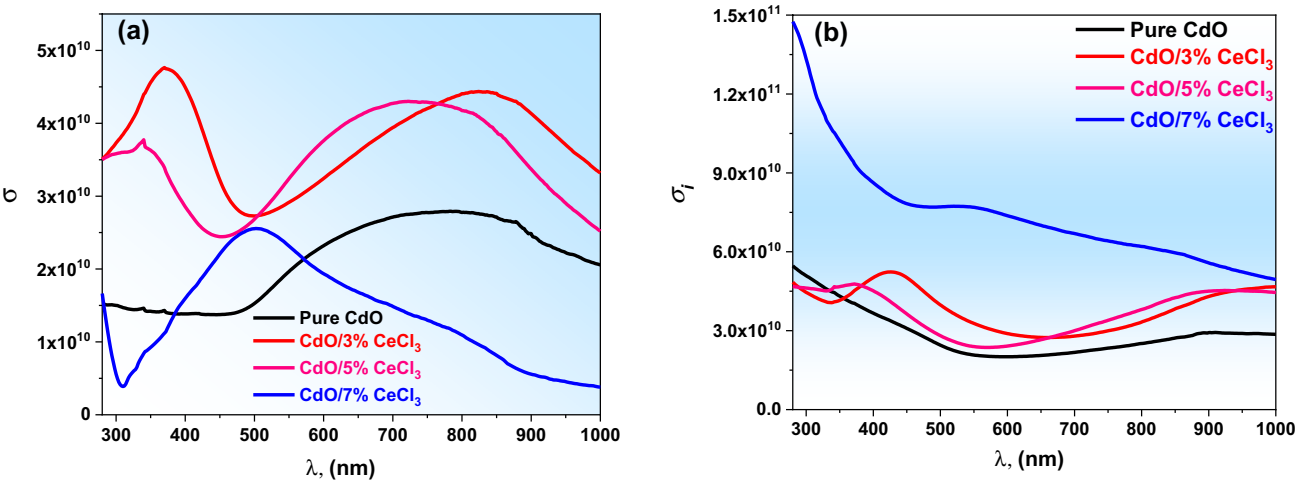

Fig. 8 **a**, **b** Optical and electrical conductivity of pure and Ce-doped (3, 5, and 7%) CdO nanostructured films

from $\sigma_e = \frac{2\lambda\sigma_{opt}}{\alpha}$. Figure 8b shows the variation of electrical conductivity of pure and doped samples. From figure σ_e is increasing the higher number of charge carriers with doping concentrations number of charge carriers available with doping percentage. Both the conductivity values are increasing with doping percentage which suggests that the present material is useful for electro-optic applications.

3.5 Nonlinear optical analysis of nanostructured Ce-doped CdO films based on the Kramers–Kronig analysis

On interaction with high-intensity laser-like light, the thin films intend to produce second and third harmonics. For lower intensities, the polarization is a linear function of the electric field; whereas, for high intensities, the polarization is a non-linear function of the electric field. Moreover, the second and third harmonic generation, higher-order refractive index has many applications in fields like communication system, display devices, optical switching device, etc. [27]. It is intended to calculate the parameters using the following equations [28, 29]:

$$\chi^{(1)} = \frac{n_o^2 - 1}{4\pi}, \tag{7}$$

$$\chi^{(3)} = A\left(\frac{n_o^2 - 1}{4\pi}\right)^4, \tag{8}$$

where A is a constant given by 1.7×10^{-10} esu [29, 30]. From the above values, the higher-order refractive index can be calculated as follows:

$$n_2 = \frac{12\pi\chi^3}{n_0}, \tag{9}$$

Figure 9a, b gives the variation of $\chi^{(1)}$ and $\chi^{(3)}$ as a function of wavelength. It is observed from the graph that the susceptibility shows an increasing tendency with the increase in doping of Ce ions. The higher-order refractive index plotted against wavelength is shown in Fig. 9c and emphasizes an enormous increase in the value of doping with Ce ions. The value has increased by an order of magnitude, i.e., from 0.5×10^{-14} esu to 1.25×10^{-13} esu.

4 Conclusion

The thin films of pure and Ce-doped CdO were prepared by the sol–gelassisted spin coating technique. Structural, morphological, linear, and non-linear optical properties of the pure and doped films are studied. XRD confirmed the polycrystalline nature and cubic structure of the films. Raman studies support XRD and reveal there are no impurities. AFM revealed the uniformity of the samples and the grain size of the pure and doped films. The transmittance of the films is about 80% and shows an increasing tendency for doping. The energy gap of the films widens over the range 2.1–4.2 e.V due to the doping of Ce ions and makes it comfortable to be used in optoelectronic devices. The dielectric constant values were also recorded for the films. Ce^{3+} possesses shielded 4f levels, which permit several well-defined

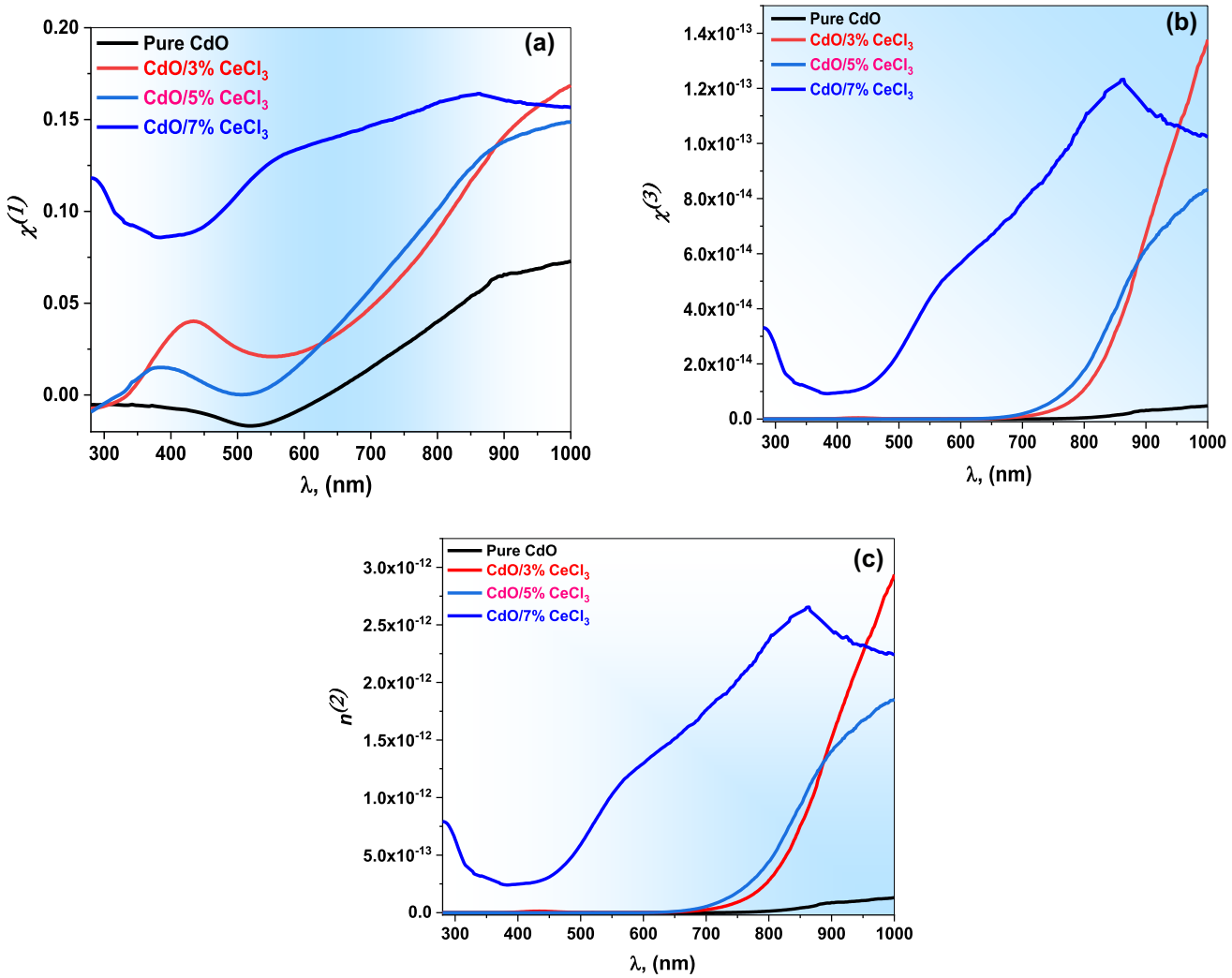

Fig. 9 **a–c** Linear optical susceptibility, third-order nonlinear optical susceptibility, and nonlinear refractive index of pure and Ce-doped (3, 5, and 7%) CdO nanostructured films, respectively

narrow optical transitions among spin–orbit levels and consequently split the bandgap of CdO into sub-gaps. For this reason, Ce^{3+} ions are generally doped or associated with CdO to enhance the luminescence efficiency by energy transfer processes, and this topic is becoming an exciting area of research for developing electronic and optical applications like sensors, light-emitting phosphors or flat panel displays. The non-linear optical properties were studied, and oscillating behavior is observed.

Acknowledgements The authors extend their appreciation to the Deanship of Scientific Research at King Khalid University for funding this work through research groups program under grant number R.G.P. 2/50/40.

References

1. A.V. Moholkara, G.L. Agawanec, K.-U. Sima, Y.-B. Kwona, K.Y. Rajpurec, J.H. Kim, Influence of deposition temperature on morphological, optical, electrical and opto-electrical properties of highly textured nano-crystalline spray deposited CdO: Ga thin films. Appl. Surf. Sci. **257**, 93–101 (2010)
2. F.F. Yang, L. Fang, S.F. Zhang, J.S. Sun, Structure and electrical properties of CdIn2O4 thin films prepared by DC reactive magnetron sputtering. Appl. Surf. Sci. **254**, 5481–5486 (2008)
3. G. Murtaza, B. Amin, S. Arif, M. Maqbool, Structural, electronic and optical properties of CaxCd1 − xO and its conversion from semimetal to wide bandgap semiconductor. Comput. Mater. Sci. **58**, 71–76 (2012)
4. S. Salam, M. Islam, A. Akram, Sol–gel synthesis of intrinsic and aluminum-doped zinc oxide thin films as transparent conducting oxides for thin film solar cells. Thin Solid Films **529**, 242–247 (2013)
5. M. Alam, M. Islam, A. Achour, A. Hayat, B. Ahsan, H. Rasheed, S. Salam, M. Mujahid, Solution processing of cadmium sulfide buffer layer and aluminum-doped zinc oxide window layer for thin films solar cells. Surf. Rev. Lett. **21**, 1450059–1450068 (2014)
6. D.A. Cristaldi, S. Millesi, I. Crupi, G. Impellizzeri, F. Priolo, R.M.J. Jacobs, R.G. Egdell, A. Gulino, Structural, electronic, and electrical properties of an undoped n-type CdO thin film with high electron concentration. J. Phys. Chem. C **118**, 15019–15026 (2014)
7. T. Singh, D.K. Pandya, R. Singh, Annealing studies on the structural and optical properties of electrodeposited CdO thin films. Mater. Chem. Phys. **130**, 1366–1371 (2011)
8. W.-M. Choa, G.-R. Heb, T.-H. Sua, Y.-J. Linb, Transparent high-surface-work-function Al-doped CdO electrodes obtained by rf magnetron sputtering with oxygen flow. Appl. Surf. Sci. **258**, 4632–4635 (2012)
9. R. Kumaravel, S. Menaka, S.R.M. Snega, K. Ramamurthi, K. Jeganathan, Electrical, optical and structural properties of aluminum doped cadmium oxide thin films prepared by spray pyrolysis technique. Mater. Chem. Phys. **122**, 444–448 (2010)
10. R.K. Gupta, K. Ghosh, R. Patel, S.R. Mishra, P.K. Kahol, Structural, optical and electrical properties of In doped CdO thin films for optoelectronic applications. Mater. Lett. **62**, 3373–3375 (2008)
11. A.A. Dakhel, Bandgap narrowing in CdO doped with europium. Opt. Mater. **31**, 691–695 (2009)
12. E. Burstein, Anomalous optical absorption limit in InSb. Phys. Rev. **93**, 632–633 (1954)
13. P. Velusamy, R. Ramesh Babu, K. Ramamurthi, J. Viegas, E. Elangovan, Structural, microstructural, optical and electrical properties of spray deposited rare-earth metal (Sm) ions doped CdO thin films. J. Mater. Sci. Mater. Electron. **26**, 4152–4164 (2015)
14. V. Ganesh, S. AlFaify, Linear and nonlinear optical properties of sol-gel spin coated erbium-doped CdO thin films. Phys. B **570**, 58–65 (2019)
15. F.F. Yang, L. Fanga, S.F. Zhang, K.J. Liao, Optical properties of CdIn2O4 thin films prepared by DC reactive magnetron sputtering. J. Cryst. Growth **297**, 411–418 (2006)
16. B.J. Zheng, J.S. Lian, L. Zhao, Q. Jiang, Optical and electrical properties of In-doped CdO thin films fabricated by pulse laser deposition. Appl. Surf. Sci. **256**, 2910–2914 (2010)
17. R. Kumaravel, K. Ramamurthi, I. Sulania, K. Asokan, Effect of swift heavy ion irradiation on structural, optical and electrical properties of spray deposited CdO thin films. Radiat. Phys. Chem. **80**, 435–439 (2011)
18. S. Jin, Y. Yang, J.E. Medvedeva, J.R. Ireland, Dopant ion size and electronic structure effects on transparent conducting oxides. Sc-doped CdO thin films grown by MOCVD. J. Am. Chem. Soc. **126**, 13787–13793 (2004)
19. A.M. Bazargan, S.M.A. Fateminia, M. Esmaeilpour Ganji, M.A. Bahrevar, Electrospinning preparation and characterization of cadmium oxide nanofibers. Chem. Eng. J. **155**, 523–527 (2009)
20. A.A. Dakhel, Transparent conducting properties of samarium-doped CdO. J. Alloy. Compd. **475**, 51–54 (2009)
21. S. Scheel, L. Knöll, D.G. Welsch, Spontaneous decay of an excited atom in an absorbing dielectric". Phys. Rev. **60**, 4094–4099 (1999)
22. A.S. Mohammed, D.K. Kafi, A. Ramizy, O.O. Abdulhadi, S.F. Hasan, Nanocrystalline Ce-doped CdO thin films synthesis by spray pyrolysis method for solar cells applications. J. Ovonic Res. **15**, 37–42 (2019)
23. P. Velusamy, R. Ramesh, K. Babu, Ramamurthi J. Viegas, E. Elangovan, Effect of La doping on the structural, optical and electrical properties of spray pyrolytically deposited CdO thin films. J. Alloys Compd. **708**, 804–812 (2017)
24. B. Sahin, Physical properties of nanostructured CdO films from alkaline baths containing saccharin as additive. SciWorldJ **172052**, 1–5 (2013)
25. H. Khallaf, C.T. Chen, L.B. Chang, O. Lupan, A. Dutta, H. Henrich, A. Shenouda, L. Chow, Investigation of chemical bath deposition of CdO thin films using three different complexing agents. Appl. Surf. Sci. **257**, 9237–9242 (2011)
26. M.M. El-Nahass, K.F. Abd-El-Rahman, A.A.M. Farag, A.A.A. Darwish, Optical characterization of thermally evaporated nickel phthalocyanine thin films. Int. J. Mod. Phys. **18**, 421–434 (2004)
27. M. Sesha Reddy, K.T. Ramakrishna Reddy, B.S. Naidu, P.J. Reddy, Optical constants of polycrystalline $CuGaTe_2$ films. Opt. Mater. **4**, 787–790 (1995)
28. S.I. Qashou, M. Rashad, A.A.A. Darwish, T.A. Hanafy, Thermal annealing effect on structural and optical properties of 2,9-Bis [2-(4-chlorophenyl)ethyl] anthrax [2,1,9-def:6,5,10-d′e′f′] diisoquinoline-1,3,8,10 (2H,9H) tetrone (Ch-diisoQ) thin films. Opt. Quant. Electron. **49**, 240–248 (2017)
29. H. Ticha, L. Tichy, Semiempirical relation between non-linear susceptibility (refractive index), linear refractive index and optical gap and its application to amorphous chalcogenides. J. Optoelectron. Adv. Mater. **4**, 381–386 (2002)
30. V. Ganesh, I. Yahia, S. AlFaify, M. Shkir, Sn-doped ZnO nanocrystalline thin films with enhanced linear and nonlinear optical properties for optoelectronic applications. J. Phys. Chem. Solids **100**, 115–125 (2017)